Surv Geophys
DOI 10.1007/s10712-012-9200-4

The Use of Resonant Orbits in Satellite Geodesy: A Review

J. Klokočník · R. H. Gooding · C. A. Wagner · J. Kostelecký · A. Bezděk

Received: 11 March 2011 / Accepted: 28 June 2012

Abstract Dynamic resonance, arising from commensurate (orbital or rotational) periods of satellites or planets with each other, has been a strong force in the development of the solar system. The repetition of conditions over the commensurate periods can result in amplified long-term changes in the positions of the bodies involved. Such resonant phenomena driven by the commensurability between the mean motion of certain artificial Earth satellites and the Earth's rotation originally contributed to the evaluation and assessment of the Stokes parameters (harmonic geopotential coefficients) that specify the Earth's gravitational field. The technique constrains linear combinations of the harmonic coefficients that are of relevant resonant order (lumped coefficients). The attraction of the method eventually dwindled, but the very accurate orbits of CHAMP and GRACE have recently led to more general insights for commensurate orbits applied to satellite geodesy involving the best resolution for all coefficients, not just resonant ones. From the GRACE mission, we learnt how to explain and predict temporary decreases in the resolution and accuracy of derived geopotential

J. Klokočník (✉) · A. Bezděk
Astronomical Institute, Academy of Sciences of the Czech Republic, 251 65 Ondřejov, Czech Republic
e-mail: jklokocn@asu.cas.cz

A. Bezděk
e-mail: bezdek@asu.cas.cz

R. H. Gooding
Surrey Space Centre, Guildford, Surrey, UK
e-mail: family.gooding@virgin.net

C. A. Wagner
Laboratory for Satellite Altimetry, NOAA, 1335 East–West Highway, Silver Spring, MD, USA
e-mail: carl.wagner2@verizon.net

J. Kostelecký
Research Institute of Geodesy, Topography and Cartography, 250 66 Zdiby 98, Czech Republic
e-mail: kost@fsv.cvut.cz

J. Kostelecký
Department of Advanced Geodesy, Czech Technical University,
Thákurova 7, 166 29 Praha 6, Czech Republic

Published online: 01 August 2012

parameters, due to passages through low-order commensurabilities, which lead to low-density ground-track patterns. For GOCE we suggest how to change a repeat orbit height slightly, to achieve the best feasible recovery of the field parameters derived from on-board gradiometric measurements by direct inversion from the measurements to the harmonic geopotential coefficients, not by the way of lumped coefficients. For orbiters of Mars, we have suggestions which orbits should be avoided. The slow rotation of Venus results in dense ground-tracks and excellent gravitational recovery for almost all orbiters.

Keywords Satellite geodesy · Earth's gravitational field · Geopotential · Orbits of Earth's artificial satellites · Resonance (commensurability) · Lumped geopotential coefficients · Fine orbit tuning · Planetary orbiters

1 Introduction, Definitions, Motivation

1.1 Phenomenon of Resonance

Resonance is the increase in the oscillation amplitude of a system exposed to a periodic force with a frequency equal or close to a natural (unforced) frequency of the system itself. Such periodic *commensurabilities* occur widely in nature and are exploited in many man-made devices. Sometimes it is a useful phenomenon (e.g., in musical instruments), but sometimes it can be dangerous and its possible presence must be accounted for in designing every building, tower, bridge, and motor car. It seems as if nature likes and often prefers resonant situations, from nuclear magnetic resonance to commensurability in celestial systems of galaxies, stars, planets (and their ring systems), and other bodies, including the Earth's artificial satellites and such curiosities as the Kirkwood gaps in the distribution of asteroids (Ferraz-Mello 1993).

1.2 Solar System Full of Resonant Relationships

Pierre Simon Laplace presented several *mémoires* on *planetary inequalities* in 1784–1786. He later dedicated *Tome Troisième* (1802) of his *Traité de Mécanique Céleste* (1825, re-edited 1878) to Napoleon Bonaparte, Citoyen Premier Consul. Laplace solved a long-standing problem in the study and prediction of the movements of Jupiter and Saturn known as the *great Jupiter–Saturn inequality*. He showed that peculiarities arose in the Jupiter–Saturn system because of the near approach to commensurability of the *mean motions* of Jupiter and Saturn. Commensurability implies resonance (from repeating conditions), that is, the mean motions are related by ratios of small integral numbers. Here, two periods of Saturn's orbit around the Sun almost equal five of Jupiter's. The corresponding difference between multiples of the mean motions, $(2n_J - 5n_S)$, corresponds to a period of nearly 900 years, and in today's terminology, we talk of 5:2 (or 5/2) orbit–orbit resonance between Jupiter and Saturn. Thanks to Laplace, the tables of the motions of Jupiter and Saturn (predictions or ephemerides) could be made much more accurate (Wilson 1985).

Since Laplace's time (particularly during the space age), many commensurabilities in the solar system have been discovered, for example, in the family of Jupiter's or Saturn's moons and rings (by interplanetary probes), among the mean motions of celestial bodies (orbit–orbit resonance), the mean motion and rotational speed of the same body (orbit-rotational resonance or orbit-spin coupling), and rotation–rotation commensurability. The phenomenon of resonance in the solar system is so frequent that we can speak of its 'resonant structure'. The resonances of natural bodies in the solar system are not the topic of this review paper, but more information on them can be obtained from, for example, Murray and Dermott (1999). Here, we focus on the orbit-rotational resonances for artificial Earth satellites and man-made planetary orbiters.

1.3 Gravitational Field of the Earth

We first introduce the *Lagrange planetary equations* (LPE), of which a standard set was given clearly by Kaula (1966), and define V, the gravitational potential of the Earth, via a spherical-harmonic expansion. The motion of any celestial body can be described by the system of differential equations known as *equations of motion*. In a general form, we can summarize them as:

$$\mathrm{d}E^j/\mathrm{d}t = \sum_i \left\{ L_i^j(a,e,I)\, \partial V/\partial E^i \right\} \tag{1}$$

where E^j is the jth *osculating* element (orbital parameter) from a standard set of six, V is the disturbing gravitational potential of the planet (as below), L_i^j (a, e, I) is a function of a (semi-major axis), e (eccentricity), and I (inclination of the orbital plane relative to the planet's equator), and $\partial V/\partial E^i$ is a partial derivative of the potential (for the case of the gravitational field in Eq. 2 specified below) with respect to the ith element. The most important element is a, being equivalent to n (mean motion) via Kepler's third law ($n^2a^3 = GM_p$, the overall gravitational constant for the planet of mass M_p).

The gravitational potential of the Earth and other roughly spherical bodies can be approximated by a spherical-harmonic expansion with Legendre's associated functions expressing dependence of the potential on geographical latitude and longitude, with *harmonic* (*geopotential*) *coefficients* (or *Stokes parameters*) C_{lm}, S_{lm} of degree l and order m accounting for the mass distribution in the body. The relevant formula is available in any textbook and will not be repeated here, though we remark that in all the older textbooks this notation applies to 'unnormalized' coefficients, with overbars added for the standard normalization; here we follow the modern practice of taking normalization for granted and dispensing with overbars. In satellite orbit analysis, it is convenient to express V along the orbit in terms of the six conventional Kepler elements (a, I, e, Ω, ω, and M) as:

$$V = \left(\frac{\mathrm{GM}}{R}\right) \sum_{l=2}^{\infty} \sum_{m=0}^{l} \sum_{k=-l}^{l} \sum_{q=-\infty}^{\infty} J_{lm} \left(\frac{R}{a}\right)^{l+1} \mathrm{Re}\left\{ F_{lm}^k(I) G_{lq}^k(e) \exp\left(i\psi_{lmkq}\right) \right\} \tag{2}$$

where $J_{lm} = \sqrt{\left(C_{lm}^2 + S_{lm}^2\right)}$, Re denotes 'real part of', R is the mean equatorial (reference) radius of the central body, $i = \sqrt{-1}$, and k and q are further integer indices, with k having the same parity as l (Gooding and Wagner 2008, 2010), so that the two lowest values of k are $-l$ and $(-l + 2)$. Finally, $F_{lm}^k(I)$ and $G_{lq}^k(e)$ are mutually independent functions of I and e, respectively (see Sect. 2.3), and ψ is the phase (in the LPEs), given by

$$\psi_{lmkq} = k\omega + (k+q)M + m(\Omega - \nu - \lambda_{lm}) \tag{3a}$$

where $m\,\lambda_{lm} = \tan^{-1}$ (S_{lm}/C_{lm}) and ν is the sidereal angle. Equation (3a) is an integrated version of the underlying formula:

$$\dot{\psi}_{lmkq} = k\dot{\omega} + (k+q)(n+\dot{\sigma}) + m(\dot{\Omega} - \dot{\nu}) \tag{3b}$$

where (for both Eqs. 3a and 3b) ω is the argument of perigee, M the mean anomaly, and Ω the right ascension of the ascending node; the time derivative of the sidereal angle is the rotational speed of the Earth. We have already introduced the mean motion, n, and from it M is defined from σ, the mean anomaly at epoch (t_0), via $M = \sigma + \int n\,\mathrm{d}t$.

For the potential V in Eq. (2), the LPEs from Eq. (1) become for the general l, m harmonic

$$\frac{\mathrm{d}}{\mathrm{d}t}\left(E^j_{lm}\right) = \sum_i \left\{ L^j_i(a,e,I) \sum_{k=-l}^{l} \sum_{q=-\infty}^{\infty} \left[J_{lm}\mathrm{Re}\left[f^{ij}_{lm}(a,e,I)\exp\left(i\psi_{lmkq}\right)\right]\right]\right\} \tag{4}$$

where f^{ij}_{lm} is a (complex) function depending on the arguments e and I in the functions G and F, respectively, or in their derivatives (G' and F'), as they affect the element specified by j.

If we integrate the nonlinear Eq. (4) in a first approximation holding all orbit parameters except M constant, the time derivative of (3a), $\dot{\psi}$ (3b), appears in the denominator and it may be that a combination of m ($\neq 0$) and $k + q$ in Eq. (3b) is such that $\dot{\psi}$ (including the orbital and Earth rotation rates) is close to zero; the small denominator is then the hallmark of an *orbital resonance*. The usual first-order analytical solution of Eq. (4), assuming constant elements on its right-hand side, then fails as it implies infinitely large oscillations in these elements as well as errors going to infinity. In practice, most satellite orbits are today integrated numerically, and the small-denominator problem hardly exists. But the linear analytical approach outlined above is very useful for quantitative estimates of small perturbations and to gain fundamental understanding of the motion.

1.4 Orbital Resonance for the Earth's Artificial Satellites

An *orbital resonance* of an artificial satellite of the Earth (or the commensurability of its mean motion with respect to the Earth's rotation) is identified by the ratio β:α, for an orbit having a ground-track repeat rate of β nodal revolutions (each from an ascending node of the orbit to the next one) over α nodal days. Here, 'nodal day' is a convenient term for the time the Earth takes for one rotation relative to the satellite's (generally moving) orbital plane. The integers α and β are co-prime (the ratio β:α must be irreducible) and define the *fundamental* resonance, but *overtone* and *sideband* resonances may also be significant. For a specific resonance, with β and α known, the ($\gamma - 1$)th overtone is specified as $\gamma\beta$:$\gamma\alpha$, with $\gamma\beta = m$, which defines the relevant values of the order m, and $\gamma = 1$ is almost always dominant (Gooding and King-Hele 1989). A sideband involves a fourth index, q, related to e, which changes the effect of $\gamma\alpha$, since $\gamma\alpha = k + q$, where k will be met again in Sects. 1.5 and 2.3.

In geometric terms, exact resonance implies a *commensurability* such that the satellite returns to the same point (above the Earth) after β nodal revolutions in α (nodal) days. In principle, the entire ground-track then repeats, but in reality the orbit experiences atmospheric drag and other perturbations, so exact resonance is an instantaneous state; we say, therefore, that the satellite passes through β:α resonance and the ground-track pattern *evolves*. As an example, Fig. 1 shows the pattern for the ERS 1 (European Remote Sensing) satellite when, during the selected phases of the mission, the satellite was placed in a 43:3 repeat orbit.

The use of a satellite's passage through orbit resonance to evaluate lumped geopotential harmonics (Sect 1.5) was pioneered by Gooding (1971a), though Allan (1965a) had already published a paper on the underlying theory, while Wagner (1965) and Allan (1965b) had

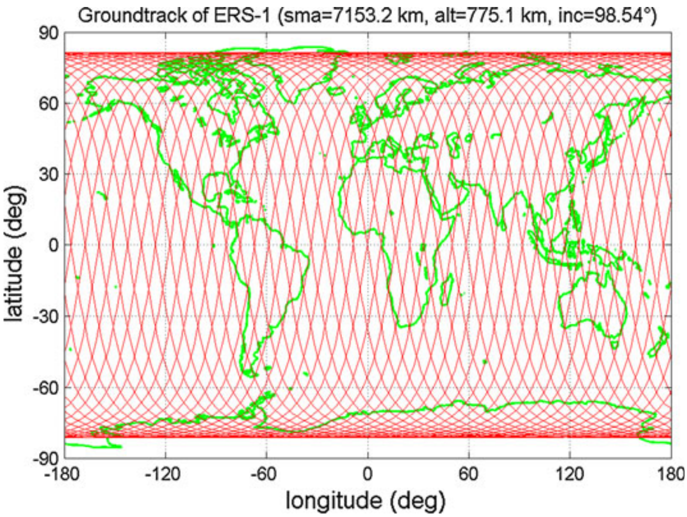

Fig. 1 The ground-track patterns of ERS 1 at exact 43:3 resonance (no drag effect considered), after completing three nodal days

published applications to the first 24-h satellite. Further papers on theory were presented by Allan (1967a, b, 1971, 1973) and Klokočník (1976), with relevant papers also by Gooding and King-Hele (1989), Wagner and Douglas (1969, 1970), Wagner (1974), and Klokočník (1979). Details from these studies are given in Sects. 2–7. The shallow resonances [e.g., Reigber and Balmino (1975, 1976), Reigber and Rummel (1978)] are mentioned in Sect. 4.

1.5 Lumped Geopotential Coefficients

The term 'lumped coefficient' refers to a linear combination of the standard harmonic coefficients for specific values of m and $k + q$, defined by β and α, plus a sequence of degrees l (all odd or all even) such that $l \geq m$ (q is zero in the simplest cases). This follows naturally from a resonant version of the standard LPE in Eq. (4), with indices (m, q) and k specified to make $\dot{\psi}_{lmkq}$ zero for l covering all the permitted values. That leads to lumped harmonics defined in the form:

$$\left(C_m^{q,k}, S_m^{q,k}\right) = \sum_l Q_{lm}^{q,k}(C_{lm}, S_{lm}) \tag{5}$$

where l increases in steps of 2 from l_0, its minimum relevant value, $k = \gamma\alpha - q$, $Q_{lm}^{q,k} = (-1)^{1/2(l-lo)}\ E_{lmq}^k / E_{lo,mq}^k$, where $E_{lmq}^k = B_l F_{lm}^k(I) G_{lq}^k(e)$ and $B_l = n(1-e^2)^{-1/2}(R/a)^l$. The symbols, other than 'E', are taken from Gooding and King-Hele (1989).

We have to bear in mind that lumped coefficients only lead to intermediate results, for later evaluation of individual harmonic coefficients, and the orbital data are not always available close to an exact resonance (see the remarks on shallow resonances in Sect. 4). Analyses of orbit inclination or eccentricity were used to compute lumped coefficients that are valid only for the particular inclination and (to a lesser extent) the semi-major axis of the orbit analysed. Then, having a set of orbits analysed for the same β:α resonance, but of as diverse inclinations as possible, we can convert the lumped values (by least-squares adjustment) into real geopotential coefficients (more in Sects. 2, 4).

The eventual goal of resonance analysis was to check and/or improve the global gravitational models of the Earth, and there are three approaches to this:

(1) Compute lumped coefficients from resonant orbits and combine them, for orbits of diverse inclinations, to get *delumped* (or ordinary) harmonic coefficients of the relevant orders, which can then be compared (as a form of calibration) with the harmonics of the global gravitational models (e.g., King-Hele et al. 1974; King-Hele and Walker 1989).
(2) Compute the lumped coefficients from the resonant orbits, but then compute equivalent lumped quantities from the global gravitational models and compare these instead of the harmonic coefficients (another form of calibration); see, for example, Kostelecký and Klokočník (1979, 1983).
(3) Get lumped coefficients, but combine them with other independent data from general satellite tracking, surface gravity, geoid heights, etc., so as to create a new global gravitational model (much more ambitious than mere calibration).

1.6 Motivation to Study Satellite Resonance in the Sixties and Seventies

Early knowledge of the gravitational field of the Earth via satellite orbits (1958–1970) was based mainly on optical and radar observations of low accuracy. King-Hele (1972) was fascinated 'with the hills and valleys of the geoid, mapped as never before…', but in fact only the basic features of the geoid were then recognized—the result was excellent for the time, but rudimentary from today's viewpoint.

Before the widespread use of laser tracking and GPS high–low satellite-to-satellite tracking, the evaluation of resonance-based lumped harmonics was often superior to that of harmonics based on scattered Doppler or precision camera observations from several non-resonant orbits, the reason for this being the amplification of the perturbations over long periods. It was a 'golden age' for orbit resonances of artificial Earth satellites (Sects. 2–4), which were used to check the validity of (or even calibrate) the published accuracies of certain parts of the global models. In some cases, they were even used directly to improve these parts of the models.

Now, however, with continuous high-precision GPS observations of satellites like CHAMP, GRACE, and GOCE (Sect. 5) dedicated to gravitational field research, resonance analyses cannot compete with high-degree global models like EGM 2008, in which the spherical harmonics are expanded to degree and order 2160 (Pavlis et al. 2008). The power of such models comes, for low-degree harmonics, almost entirely from the GRACE low–low intersatellite data while, for high-degree ones, it comes from the data associated with surface-gravity anomalies, either directly observed or inferred (partly) from satellite altimetry. Thus, as will be seen in Sects. 7–9, the role of satellite resonance today is rather different from its original one.

2 Study of Satellite Resonance at RAE, Farnborough, England

2.1 Origins

The satellite Ariel 3 (the first one to be built entirely in the UK) was launched for the Royal Aircraft Establishment (RAE) on 5 May 1967, with experiments for the RAE's Space Department. The satellite was tracked by NASA's Minitrack Network, but the definitive orbit determination (based on the resulting interferometer data) was carried out at RAE. Routine publication of the orbital parameters, at three-day intervals, drew attention to the entirely unexpected variation of the mean inclination (to the Earth's equator) over a roughly three-month period from mid-December (1967). The behaviour consisted in a marked (and steady) decrease of about 0.02° (from 80.18° to 80.16°), swamping the lunisolar perturbations that had been expected to be the most significant ones and which were evaluated by a computer program. The lunisolar effects, however, were compounded of purely periodic perturbations, and the only expected *secular* perturbation was the one due to atmospheric rotation, the effect of which was eventually evaluated to be $(-8.0 \pm 0.6) \times 10^{-6}$ deg/day (Fig. 2).

In due course, it was realized that the unexpected decrease in inclination was due to the 15:1 resonance between the satellite's orbital period and the 15th-order harmonics of the geopotential. The key quantity for Ariel 3 was perceived as the resonant angle, Φ_{15}, given by

$$\Phi_{15} = \omega + M + 15\,(\Omega - \nu) \tag{6}$$

where ω, M, Ω, and ν have already been introduced for Eq. 3a. (Φ_{15} was eventually generalized to ψ_{lmkq}, the change from Φ to ψ being to permit the inclusion of λ_{lm} in the equation.) The dominant (secular) variations in the RHS of Eq. (6) arose from M and ν, because the (fixed) rate of ν is about 361 deg/day, while Ariel 3 happened to be launched to a height at which M was initially increasing at nearly 15 times this rate, it was only a matter of time before the ratio was, for an instant, exactly 15:1 (M's acceleration is due to the satellite's gradual height loss). The 'instant' occurred on 3 February 1969.

The symmetric behaviour, relative to the satellite's passage through exact resonance, of the orbital inclination is clear from Fig. 2, taken from Gooding (1971a), where the raw values (from the interferometry data) are plotted, as well as the theoretical least-squares fit of four parameters to 281 equations of condition; these parameters were two lumped harmonic coefficients, denoted by C_{15} and S_{15}, together with a pair of linear parameters I_0 and $\dot{I}$. The inclusion of two other parameters was tried, viz. the 'first-overtone harmonic harmonics' C_{30} and S_{30}, but the data were inadequate for the significant derivation of these parameters in addition to the other four. The lumping for C_{15} consisted just of a linear combination of $C_{15,15}$ itself, $C_{17,15}$, $C_{19,15}$, and $C_{21,15}$, and similarly for the lumping of S_{15},

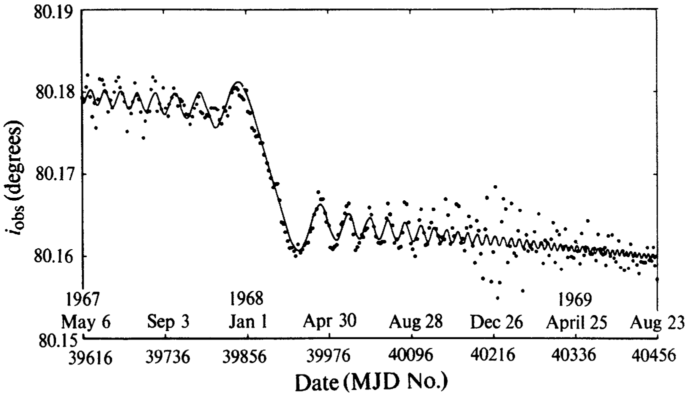

Fig. 2 Inclination variation of Ariel 3 through 15th-order resonance, from 3-day orbit determination followed by analysis for lumped coefficients (reproduced from Gooding 1971a)

but delumping of C_{15} and S_{15} was impossible until additional equations (for similar linear combinations of lumped C_{15} and S_{15}) could be obtained from satellites in orbits with significantly different inclinations (because Q_{lm} from Eq. 5 depends strongly on the inclination). The first simultaneous analysis (by least squares) of a number of lumped harmonics for $m = 15$, with l odd and ≥ 15, was published by King-Hele et al. (1974)—it led to nine pairs of 'unlumped' harmonic geopotential coefficients from odd-m up to $l = 31$, after the use of 11 satellites.

2.2 Development

The obvious direction for development was to use satellites in orbits of different inclinations to obtain different 'lumpings' of actual harmonic coefficients and hence to obtain (by the least-squares solution of elementary linear equations) individual values for these coefficients (inseparable without the individuality of the inclinations). King-Hele (at RAE), closely followed by Kozai (at the Smithsonian Institution Astrophysical Observatory, SAO) and others, had already used this technique for the zonal harmonics, needing to analyse those of even and odd degree separately.

That need carried through to the separation of the even and odd degrees for the harmonics of order 15 (and other orders when analysed), and also (of course) for the lumped degrees, so several RAE analyses of order-15 resonance-based lumpings were made, with King-Hele and Walker (1989) eventually giving values for degrees up to 36 (both odd and even). Table 6.2 of King-Hele's book (King-Hele 1992) gives only a sample of the complete values. An interesting 15th-order resonance graph appears in the book as Fig. 5.6., and here as Fig. 3, interesting because it is e (not the far more usual I) that is plotted.

2.3 Inclination Functions

The inclination F-functions, mentioned earlier, were introduced by Kaula (1966), using a third subscript p rather than the superscript k (Gooding and Wagner 2010) used throughout this paper. Their function is to assist in the transformation of geopotential-related

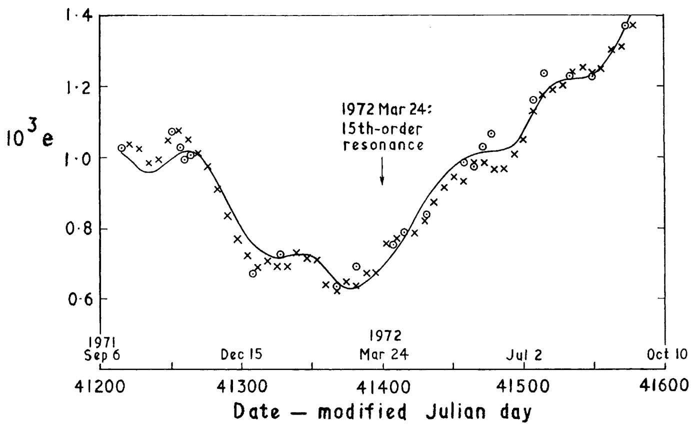

Fig. 3 Values of eccentricity for Cosmos 395 rocket at 15th-order resonance, with fitted theoretical curve (reproduced from King-Hele 1992)

quantities from an equator-based coordinate system to one based on the orbital plane of a particular satellite under study. The functions were soon recognized as essential to orbit theory, and Allan (papers from 1965 to 1973) was the RAE's main theoretician in this area. He followed Kaula's basic formula (with modifications) but initiated what became a standard recurrence relation (Gooding 1971b) as a better way for efficient computation. But this way to compute F is not the best possible, as two of the present authors have shown in their recent papers (Gooding and Wagner 2008, 2010).

Other work on the inclination functions came from Kostelecký (1985), Kostelecký et al. (1986), Sneeuw (1992), and others (all outside RAE); it had become necessary to compute the inclination functions to very high degree, and the basic formula of Kaula and Allan was not numerically stable, with eventual underflow or overflow at some degree. In important work, Risbo (1996) showed how F could be computed in an entirely different way, via recurrence superimposed on convolution, and this was developed further by Gooding and Wagner (2010).

2.4 Book by Desmond King-Hele

A section summarizing the main contributions of RAE's Space Department would not be complete without more general reference to the book (King-Hele 1992), cited in a particular context at the end of Sect. 2.2. This was effectively the culmination of an astonishing output of research and publications in which Dr. King-Hele, F.R.S., contributed to many aspects of satellite orbits, with resonance one of the topics he studied most.

3 Study of Resonance at GSFC NASA

In the USA, resonances were studied at many institutions, mainly in the 1960s prior to and after the first 12- and 24-h communications satellites (in 2:1 and 1:1 resonances) were operational (e.g., Blitzer et al. 1962; Wagner 1965; Kaula 1966, chapter 3.6; Garfinkel 1966; Gedeon et al. 1967; Murphy and Victor 1968). The first actual applications of these resonant orbits to satellite geodesy were not through the lumped coefficients for high-order resonances of low orbits (Sect. 2) but rather from direct observations of their mean longitude accelerations (see also Allan 1965b; Wagner 1968a, b). Each of these accelerations in general involves more than a single order (m) and kind (C and S), for example, Kaula ibid (Eq. 6.12).

Later, to study the much longer free drift of these and lower-altitude resonant orbits (some subject to atmospheric drag), a semi-numerical Resonant Orbit Analysis and Determination (ROAD) program was developed (Wagner and Douglas 1970). The numerical part was the integration of the LPEs but the analytic part was only for selected long-term effects in the potentials of the Earth, Sun, and Moon, including radiation pressure and drag. The ROAD program achieved a speed of roughly 100 times a full numerical integrator. It could cover the complete passages through multiple resonances, the shallow ones included.

Many of the objects/orbits used in these studies were 'discovered' by examining the GSFC Satellite Situation Reports (Wagner and Douglas 1969). The results (to the mid-1970s) for resonant orbits (both circular and highly eccentric) of 1–15 revolutions/day, including the use of the observed resonant observations in testing the accuracy of global gravitational fields determined from independent data, are given in Wagner and Lerch (1978). See also: Wagner (1968a, b, 1973), Wagner and Klosko (1975, 1977).

With satellite altimetry coming on the scene, it was clear that gravitational models were not of sufficient accuracy, but satellite altimetry data improved them enormously. The main problem was to distinguish the geoid and permanent sea surface topography in the altimeter observations. Wagner (1983) tested the models of that time (GEM 9, GEM L2, and GRIM 3), from either independent satellite observations or the prior computation of lumped coefficients from 1:1 resonances. He found that the geoid errors from the models permitted the resulting topography to be 'visible' at long wavelengths, though radial orbit errors in the altimetry remained an obstacle, resolved only by improved models. This topic has been intensively studied during the last two decades by Klokočník et al. (2008b).

4 Study of Resonance in Continental Europe

Using tracking data for stable near-resonant orbits of 12th, 13th, and 14th orders, a German–French team applied generalized Fourier analysis to longer-period resonance perturbations (typically covering several days) in mean longitude, inclination, and eccentricity (Reigber 1973). Condition equations, for whichever order, were derived, largely for use in assessing global GRIM models (Balmino et al. 1976; Reigber and Rummel 1978). Individual resonance terms, for each order, were derived from these observation sets by a generalized least-squares method known as collocation (Reigber and Balmino 1976), largely for intercomparison with RAE and GSFC results.

The theoretical background of the method was developed at TU Munich (Schneider 1973) and applied numerically, for example, by Reigber and Balmino (1975, 1976) for the 13th and 14th orders and by Reigber and Rummel (1978) for the 12th order (using non-homogeneous weight functions). The resonance results were then compared with those from the current global gravitational field models of the time, an application of many of the results being to calibrate the models. We should also recall the work of Hugentobler et al. on the 2:1 and 1:1 resonances, for example, in Hugentobler and Beutler (1993) and Hugentobler et al. (1999), and also the activities of COGEOS (Interntl. *C*ampaign of Optical *O*bservations of *Geo*synchronous *S*atellites for Geophysical Purposes), for example, Nobili (1993).

King-Hele (1992) mentions the cooperation of the United States, UK, and Czechoslovakia in the days when it was not even easy to exchange letters between the 'socialist paradise' and its 'capitalist enemies' (with no email or Internet of course). Every letter to or from the Astronomical Institute of the Czechoslovak Academy of Sciences in Ondřejov had to be checked by the vice-director of the Institute. Nevertheless, very friendly correspondence and cooperation were possible. Czechoslovakia received NASA's Technical Reports and RAE Technical Reports, thus obtaining valuable information. Klokočník met King-Hele and Doreen Walker in person at Lagonissi, Greece, in 1977 (during the conference 'Artificial satellites for geodesy and geodynamics'). Gooding visited Prague and Ondřejov for the first time in 1980, after the COSPAR General Assembly in Hungary, and Klokočník's first US visit to the Wagners was in 1992, but Klokočník and Wagner were both already working on satellite altimetry by that time.

Czech studies started with some resonance theory (Klokočník 1976), following the work at Farnborough and Goddard, and Klokočník (1988) later extended the theory. A group in satellite dynamics at the Ondřejov observatory of the Astronomical Institute under the leadership of Ladislav Sehnal developed the computer program PRIOR (Lála and Kostelecký 1980) for analytical orbit determination. It was based on camera and laser observations, following the theory and code for the US DOI (Differential Orbit Improvement) program (Gaposchkin 1964). But there was a paucity of precise observations for several

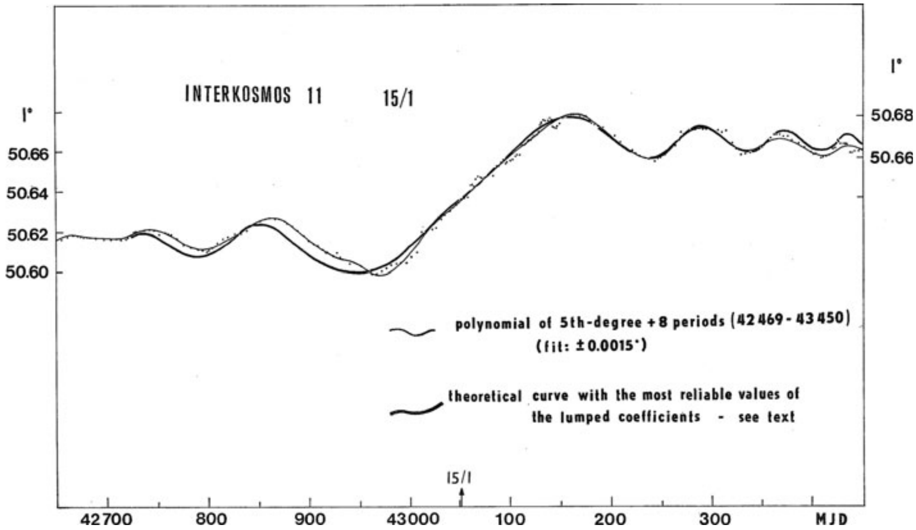

Fig. 4 Inclination variations of Intercosmos 11 at the 15th-order resonance, 15:1, reproduced from Klokočník (1979), analysed for the 15th- and 30th-order lumped coefficients

interesting satellites that passed through 15th-order resonance, including Intercosmos 9, 10, 11, 14, and 17, as well as the first Dutch satellite, ANS 1; Wakker et al. (1981); so orbits were either provided by the Astrosoviet network (USSR) or taken from the Two-Line Elements of NASA.

The most successful analysis was that of Intercosmos 11's inclination, which suffered the large change of 0.08° from resonance, corresponding to about 10 km cross-track (Klokočník 1979), which was published before RAE (Walker 1981). The inclination behaviour of Intercosmos 11, around the 15:1 resonance, is shown in Fig. 4. The lumped coefficients computed in Ondřejov were included as additional condition equations in the German–French GRIM 3 Earth model (Klokočník and Kostelecký 1981).

Some success was also achieved in the adjustment of individual 30th-order harmonics from lumped coefficients (Kostelecký and Klokočník 1983), by applying collocations, see Moritz (1980). The collocation accounts for the statistical behaviour of a signal, amounting to an assumed observation of zero for an unknown harmonic, with uncertainty given by Kaula's rule for the geopotential's decline with degree, as estimated from the autocovariance analysis of gravimetry (Kaula 1966, p. 98).

5 CHAMP and GRACE: Revived Use of Resonance

5.1 Satellites CHAMP, GRACE, and GOCE

All three satellites were designed to study the fine structure of the Earth's geopotential field. For information about their missions, see, among others, Reigber et al. (2003, 2005) for CHAMP, Tapley et al. (2004) for GRACE and ESA (1999), or Floberghagen et al. (2012) for GOCE. We also recommend www.gfz-potsdam.de.

CHAMP (CHAllenging Minisatellite Payload for geophysical research and application, GFZ/DLR, Germany) was launched in summer 2000 (with $I = 87.3°$) and was active till September 2010.

GRACE (Gravity Recovery And Climate Experiment, NASA/DLR) was launched in spring 2002 and is still active. It consists of two near-identical satellites in (effectively the same) low near-polar orbit, separated by a distance of about 220 km. Accurate measurements of variations in this distance, due to the geopotential field, lead to the determination of its coefficients.

GOCE (Gravity field and steady-state Ocean Circulation Explorer, ESA) was launched in spring 2009 and is still working in an extremely low circular nearly polar orbit. For the first time ever, a satellite was equipped with a space gradiometer (consisting of 6 micro-accelerometers) able to 'measure' the full Marussi tensor (tensor of the second derivatives of the disturbing geopotential). The actually achieved accuracy is 10 milliEõtvõs/Hz$^{1/2}$ (1 E $= 10^{-9}$ s^{-2}), but not the same (so high) for all components of the tensor (10 mE/Hz$^{1/2}$ for V_{xx} and V_{yy} while 20 mE/Hz$^{1/2}$ for V_{xz} and the others, surprisingly including V_{zz}) (see Rummel et al. 2011). Each additional measurement cycle (2-month intervals) improves the accuracy (and also the resolution) of the geopotential coefficients derived from the measured gradients.

For all these missions, the choice of orbit is crucial. Gravitational field missions are preferably placed in low near-circular repeat orbits to ensure consistent high sensitivity to the gravitational signal. Very important also is the choice of inclination I, the orbit often being selected as near-polar (for global coverage) and retrograde to be Sun-synchronous (involving $I \sim 98°$) to ensure a constant illumination of the satellite's body by sunlight.

5.2 Diagrams for Resonance Evolution

For the exact resonance $\beta{:}\alpha$ and the phase ψ_{lmkq} (Eq. 3a) in the LPE, we have $\dot{\psi}_{lmkq} = 0$ (Eq. 3b). The relevant satellite mean motion n can then be expressed as:

$$n = \frac{\beta}{\alpha}\left(\dot{\nu} - \dot{\Omega}\right) - \dot{\omega} - \dot{\sigma}_0 \tag{7}$$

where $\dot{\Omega}, \dot{\omega}, \dot{\sigma}_0$ are numerically much smaller than $\dot{\nu}$ and dominated, from Eq. (2), by the Earth's oblate coefficient. We can illustrate the situation by taking the LPEs for the individual elements Ω, ω, and σ_0, just to see the largest perturbation effect, which is due to $J_2 = -\sqrt{5}\,C_{20}$ (J_2 is not $J_{2,0}$ from Eq. 2). Then, Eq. (7) gives us (Allan 1973; Wagner 1991; Klokočník et al. 2003, 2008a; Bezděk et al. 2009):

$$n = \frac{\beta}{\alpha}|\dot{\nu}|\left\{1 - \frac{3}{2}J_2\left(\frac{R}{a}\right)^2\left(4\cos^2 I - \tau\frac{\beta}{\alpha}\cos I - 1\right)\right\} \tag{8}$$

where $\dot{\nu} > 0, \tau = 1$ applies to direct normal rotation, and $\dot{\nu} < 0, \tau = -1$ to retrograde rotation (applying, in particular, to the planet Venus, as may be seen from Table 1 in Sect. 8).

We note that Eq. (8) is a generalized equation for the mean motion (n) in a commensurate orbit, but we will not go into details such as the specific a (as a function of I) that should be used. For discussion of that, and further consideration of this topic, see Klokočník et al. (2003).

The 'resonance evolution diagrams' in Figs. 5, 8, 11, 14, and 16 should now be clear. On the x-axis, we have the integer α, and on the y-axis, we have a (or height $h = a - R$). Each graph point corresponds to a resonance and is labelled either $\beta{:}\alpha$ or just β. The graphs are valid only for the particular I and a range of a (or h), the results being valid for (effectively) circular

Table 1 Basic parameters of the Earth and other bodies of the solar system

Body	GM ($km^3\ s^{-2}$)	J_2 (10^{-6})	R (m)	$\dot{\nu}$ (rev/day)
The Earth	398,600.44	1,082.627	6,378,137	1.00274
The Moon	4,902.80	203.428	1,738,140	0.03660
Mercury	22,032.24	60	2,439,700	0.01705
Venus	324,858.36	5.97	6,051,800	−0.00411
Mars	42,828.37	1,959.2	3,396,190	0.97470

orbits (significantly eccentric orbits of a planet with a deep atmosphere are generally not optimum for gravitational field studies; however, see, for example, Wagner 1979).

As time passes, a is reduced by drag and the orbit passes through the resonances from top to bottom (y-axis) as shown in Fig. 5. Note that at every moment we are inevitably close to a resonance, but for most of the time, the nearest ones are of high order (large β and relevant $\beta{:}\alpha$) and have no practical application from the viewpoint of either gravitational field study or oceanography.

Such a 'resonance evolution diagram' was first generated at DGFI Munich when some of us were cooperating on the orbit choice of the ESA altimetry mission ERS 1 (Reigber et al. 1988). It replaced the alternative graphical representation used at the time (e.g., Lefebvre and Vincent 1988). Our method of representation is now widely used (e.g., Capderou 2005).

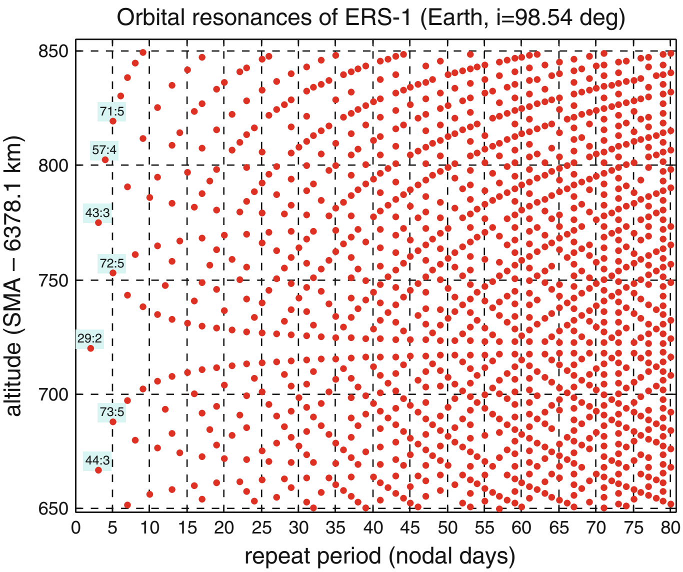

Fig. 5 'Resonance-diagram' for ERS 1 ($I = 98.54°$). The first phase of its flight was kept at the 43:3 resonance (the commissioning phase and phase for oceanography), then the orbit was manoeuvred to a bit lower to the 502:35 resonance for other oceanographic applications (kept in the given orbit with about 1 km wide window in altitude), then again to 43:3 (the so-called ice phase) and finally was free falling for geodetic applications (study of detailed marine geoid from altimeter measurements)

Resonance evolution diagrams show which resonances would be met during the free fall of a satellite from its initial orbit with a given inclination and height range (from the values of a), or which exact repeat mission of a constant height should be selected for oceanography. But they can also suggest which orbits should be avoided, as in the cases of GOCE and planetary orbiters used for gravitational potential recovery (Sects. 7, 8).

It is useful to define (and use but with care to avoid misunderstandings) the term *density of the ground-tracks at the equator*, by *1/D*, where $D = 2\pi R/\beta$, in (km), originally according to Farless (1985), where the Earth's circumference $2\pi R$ is 40,075 km, consistent with $R = 6\ 378.134$ km (as implied by Sect. 1.3). The quantity D can be understood as the longitudinal spacing (distance) of adjacent (in the same sense, or ascending or descending) satellite tracks at the equator, after the relevant repeat period has elapsed. We will use D in Sect. 6, but in Fig. 8b (also Sect. 6), we show the ground-track spacing as the maximum distance between the tracks, at different latitudes, from the actual orbit (it is not this D).

5.3 Use of Resonances with CHAMP and GRACE

Analysis of CHAMP's long-term variation in I and Ω in 2002–2007, during which (thanks to orbit manoeuvres) it passed through the 31:2 resonance three times and twice through 47:3 (Fig. 6), has yielded precise values for pairs of lumped harmonics of 31st and 47th order, and the overtones ($\gamma > 1$) of 62nd, 93rd, and 94th orders. The majority of the values of these orders were superior in precision to projections from all comprehensive global gravitational models prior to 2002. They show that, for the most part, the errors in the medium- to high-order terms for the older models and the best from CHAMP-only tracking are well calibrated. Our analyses were presented by Klokočník et al. (2003), and Gooding et al. (2004, 2007).

The essence of resonance analysis is the least-squares determination of the relevant pairs ($C_m^{q,k}$ and $S_m^{q,k}$) of the lumped harmonics and any other necessary parameters, by fitting

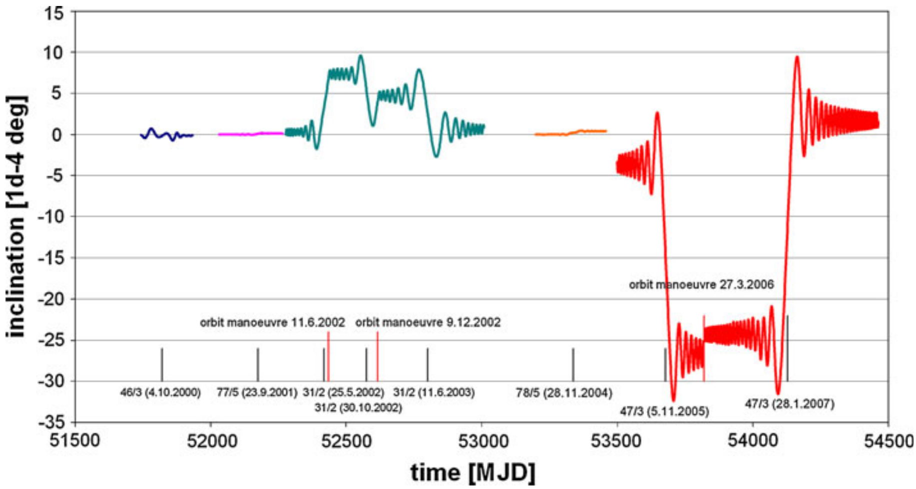

Fig. 6 Inclination changes of CHAMP (computed with the gravity field model Eigen-3p) during the 46:3, 77:5, 31:2, 78:5, and 47:3 resonances in some cases repeated due to the fact of the orbit manoeuvres. Equivalents of maximum resonance orbit changes expressed in metric scales are ~50 m for the 31:2 and ~150 m for the 47:3. Reproduced from Gooding et al. (2004)

the orbital elements or state vectors over a significant period (weeks or months) around the exact resonance; the objective of the fit is to extract maximum information from the (one or more) passage(s) through the resonance. Either before fitting, or as part of it, the data should be cleaned (as far as possible) of other long-period non-resonant effects on the satellite's orbit—in particular due to the Earth's zonal harmonics, direct lunisolar attraction, tides (both solid and ocean), atmospheric drag, precession and nutation, and solar radiation pressure. For high accuracy with the orbits of CHAMP and GRACE (in contrast to earlier resonant orbits), this is not a trivial task (Gooding et al. 2007).

As an example of the lumped coefficients, from the inclination of CHAMP at the 31:2 resonance, we found for $C_{31}^{0,1}$ (similarly $S_{31}^{0,1}$):

$$\begin{aligned} C_{31}^{0,1} &= C_{32,31} + 0.910\, C_{34,31} + 0.740\, C_{36,31} + 0.567\, C_{38,31} + \ldots \\ &= (-16.70 \pm 0.14) \times 10^{-9} \end{aligned}$$

while at the 62:4 overtone, we found for $C_{62}^{0,2}$ (similarly $S_{62}^{0,2}$):

$$C_{62}^{0,2} = C_{62,62} + 0.608\, C_{64,62} + 0.456\, C_{66,62} + 0.363\, C_{68,62} + \ldots = (3.02 \pm 0.03) \times 10^{-9}$$

In both cases, the series are for even l's, as a consequence of $\gamma\alpha + q$ (with $q = 0$) being even. This was explained by, for example, Allan (1973) and has further important consequences here. Thus, with l–m odd for 31:2, the variation of I (for $q = 0$) is close to minimum, while for 62:4, with l–m even, it is close to maximum. This accounts for the superior resolution of the 62nd-order effect seen above. On the other hand, the situation for the main variations of Ω (for $q = 0$) is reversed, because the nodal variations are controlled by the derivatives of the I-governing inclination functions and not the inclination functions themselves.

Staying with the CHAMP 31:2 resonances, three pairs of order-31 harmonics (for $q = -1$, 0, 1) were derived from the triple resonance passage (Fig. 6 again). The first-overtone harmonics (with $m = 62$) were important for I, because (for $q = 0$, l–m being even, and a near-polar orbit) they involved near-maximum effects.

Turning to 47:3, Fig. 6 shows that CHAMP passed through the fundamental I-resonance twice and its first overtone (94:6) once. The two main resonances, one fundamental and the other the first overtone, permitted resolution by the fact that the $(l - m)$-terms in both cases are even.

Regarding the resonances of GRACE (A and B), both satellites passed slowly through 61:4 in the autumn of 2004 (Wagner et al. 2006). With even the fundamental order (as well as the altitude) so high, however, the effect on I was seen only poorly from the mean orbital data available, but the lunisolar effects (computed by numerical integration) were strong enough to be visible, while the radiation-pressure effects were insignificant compared with data errors.

Numerical results from CHAMP as well as GRACE may be seen in Gooding et al. (2007). The same applies to comparisons of the resonant results with the global gravitational field models published at the time.

6 Found via GRACE: Accuracy of Geopotential Models Versus Ground-Track Density

Satellite-to-satellite tracking between GRACE A and B has been used to determine monthly solutions (or even 10-day solutions) for the geopotential and hence its variation with time (Tapley et al. 2004; Bettadpur and team 2006; Bruinsma et al. 2010; and others).

The change in individual static field solutions for each month (or another regular time interval) yields the change in the field on the basis of the chosen interval as a step. The monthly solutions became operational GRACE products provided by the 3 GRACE processing centres at UTC, JPL, and GFZ (e.g., Flechtner et al. 2010). Notes on the different releases and the different releases themselves are available online routinely at the PO.DAAC/JPL and ISDC/GFZ data centres.

It happened that the accuracy of these results suddenly decreased in the autumn of 2004 (Fig. 7a), though the method, data accuracy, and processing remained unchanged. After that autumn, the accuracy increased again—to the original level. This phenomenon of the accuracy variation has been described and explained by Wagner et al. (2006), being the consequence of GRACE's encounter with the 61:4 commensurate orbit, leading to a temporary but significant decrease in ground-track density.

Due to orbital decay from the atmosphere, a similar situation was likely to occur for GRACE in other encounters with resonance commensurabilities; see the evolution and 3D diagrams (based on real orbital elements) in Figs. 8a and b. Indeed, in 2010 GRACE passed through the 107:7 resonance and a temporary decrease in effective geopotential field resolution was registered again, similar to 61:4 in 2004 (Fig. 7b, Bettadpur 2010, priv. commun.), but this being a weaker resonance, its effect was smaller.

The core of the phenomenon of accuracy decrease can be described as follows. At a low-order resonance (when β is small, say 15, 31, or 47), the value D is much larger (by orders of magnitude) than in the more 'general' case (with, e.g., a high-order commensurability of $\beta \sim 200$): compare, for example, Fig. 9a with b and (later) Fig. 15a with b. Then, we can have the same number and quality of satellite observations for gravitational field determination, though the density of the ground-tracks at the equator and with respect to both latitude and longitude is much less (it means the value D is much higher) for Fig. 9b than for Fig. 9a.

Note, however, that the phenomenon is only temporary (Fig. 7a); due to the atmospheric drag, the semi-major axis of the satellite steadily decreases, so D changes significantly with time in a free falling orbit of low to moderately low altitude. After a while, the accuracy returns to its pre-resonance level (e.g., Fig. 7a, year 2005), because D goes back to its earlier level, but a new (low-order) resonance may appear later and the phenomenon of accuracy decrease will again be annoying (e.g., 107:7, Fig. 7b, and 46:3 or 31:2 in the future, Fig. 8a).

To avoid reduction in the accuracy of the gravitational field parameters, we may want to choose a commensurate orbit where β is higher than the maximum degree $l_{\max}$ of the harmonic expansion wanted for the particular body's resolution. This choice will introduce some correlations between orders but has an advantage of smaller truncation for the larger permitted field. The more conservative limit $l_{\max} < \beta/2$, proposed by Colombo (1983) and proven as m-correlation free by Wagner et al. (2005, 2006), is still being discussed, for example, by Weigelt et al. (2009), and more (in preparation).

For GRACE and its 61:4 resonance, the conservative limit $l_{\max}$ is severe, restricting the retrievable degree to a mere 30! Even if the rule would not be $l_{\max} < \beta/2$ but $l_{\max} < \beta$ (Weigelt et al. 2009), we know that for the Earth we achieved $l_{\max} \sim 2{,}000$ in the recent combined gravity models and $l_{\max} \sim 200$ in satellite-only models. Thus, the low-order resonances such as 61:4 (and similar ones which GRACE already has met or will meet during its decay in the atmosphere, such as 107:7) will remain a problem. The authors of gravitational field determinations from GRACE may want to resolve them to much higher degree and order for the high resolution now needed in geo-applications. But there is no

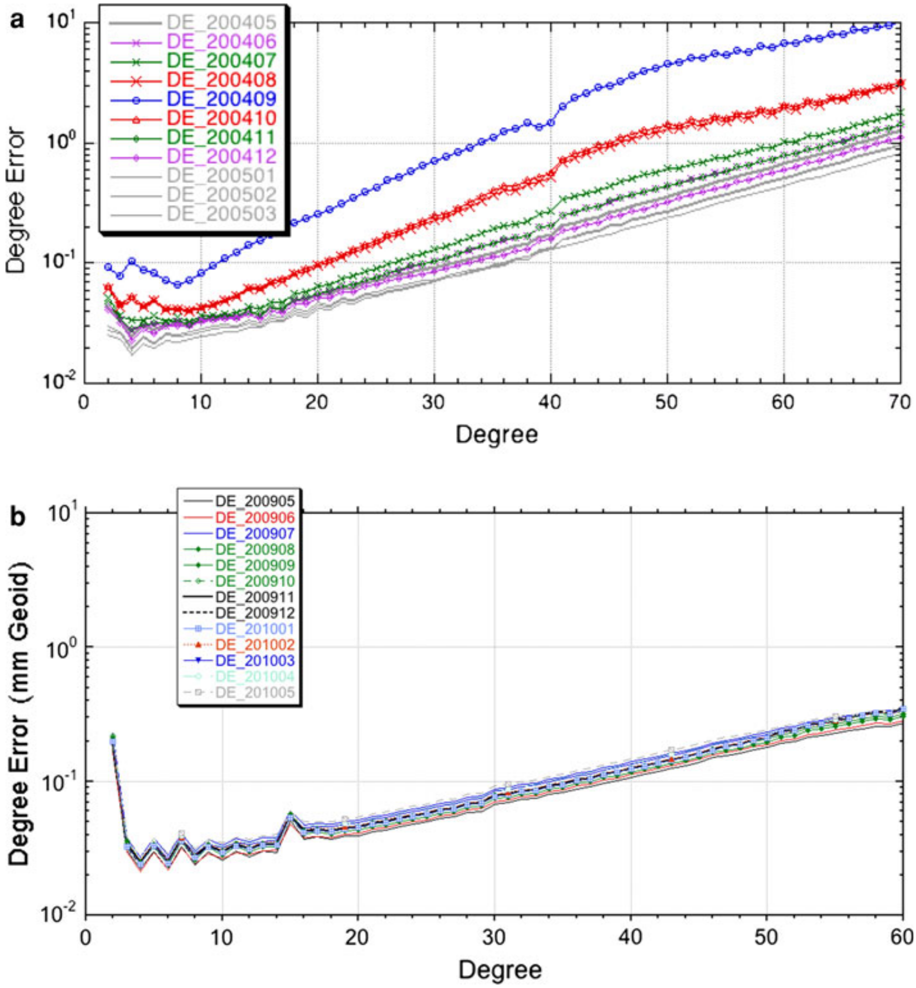

Fig. 7 **a** Accuracy of the monthly solutions for the geopotential variations from GRACE A/B data, courtesy of S. Bettadpur (2004, 2006, priv. commun.), from May 2004 to March 2005. Note the remarkable accuracy decrease between August and October 2004. On the *x*-axis, there is degree of harmonic expansion of the gravity field variations. Note the logarithmic scale on the *y*-axis with the error of geoid height in millimetres. The accuracy decrease has been explained by temporary presence of the 61:4 orbit resonance (Wagner et al. 2005, 2006). Here was the inspiration for further studies of relationship between the resonance, ground-track density, and accuracy of gravitational parameters. **b** Accuracy of the monthly solutions for the geopotential variations from GRACE A/B data, courtesy of S. Bettadpur (2010, priv. commun.), around the 107:7 resonance, from May 2009 to May 2010

way to remove low-order resonances from the orbit of a freely falling satellite, and we have to allow for temporary drops in accuracy.

Detailed analyses about the relationship of the low-order resonances, ground-track density changes, and the accuracy of the gravitational field parameters derived from such orbits have been published in Klokočník et al. (2008b) and Weigelt et al. (2009).

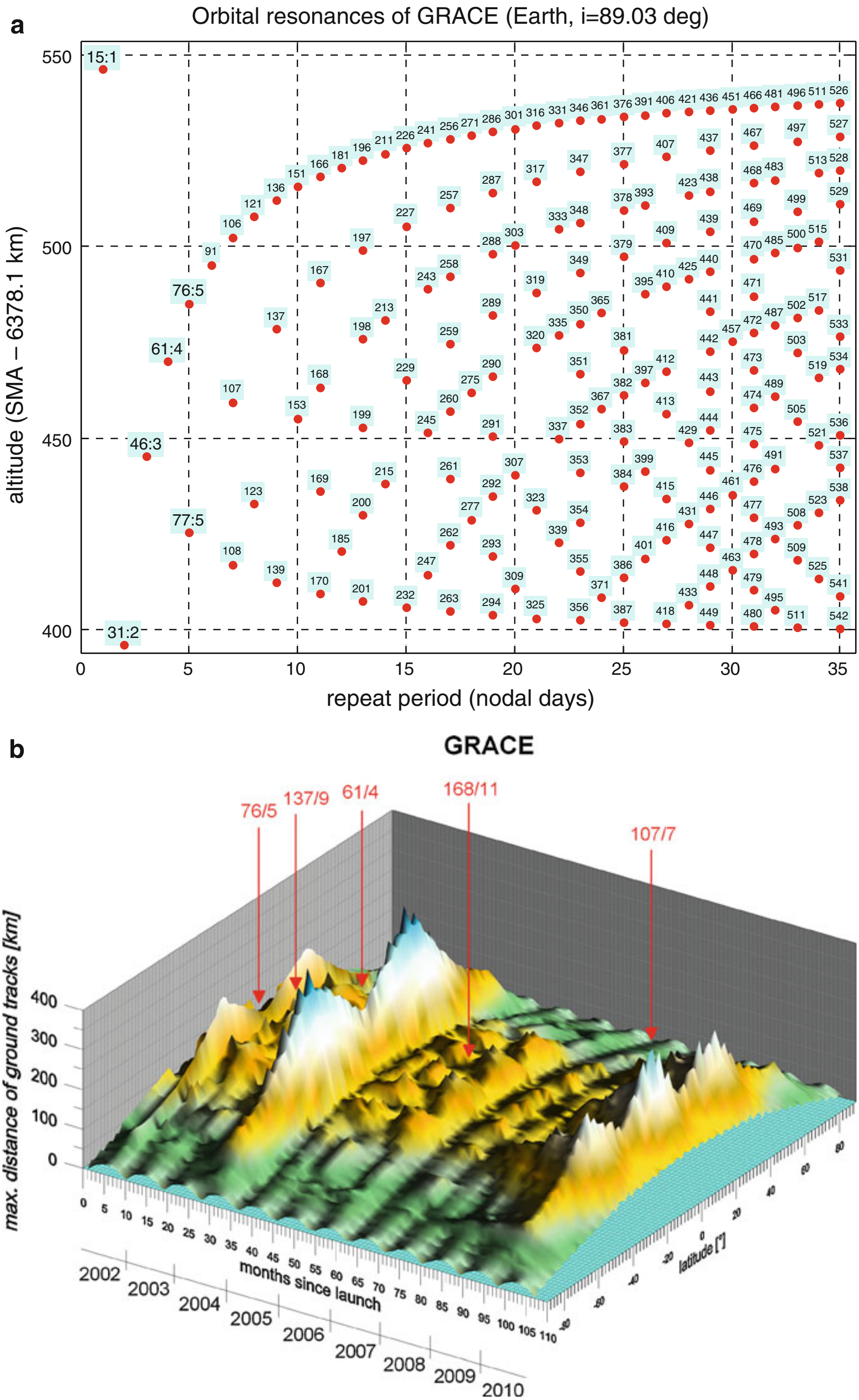
a
Orbital resonances of GRACE (Earth, i=89.03 deg)
altitude (SMA – 6378.1 km)
repeat period (nodal days)
550
500
450
400
0
5
10
15
20
25
30
35
15:1
76:5
61:4
46:3
77:5
31:2
b
GRACE
76/5
137/9
61/4
168/11
107/7
max. distance of ground tracks [km]
400
300
200
100
0
months since launch
latitude [°]
2002
2003
2004
2005
2006
2007
2008
2009
2010

◀ **Fig. 8** **a** Evolution of resonances for free fall of GRACE A/B satellites since their launch (2002). Till 2011, the satellites passed through the 61:4 and 107:7 resonances; the 46:3 and 31:2 will be the next lowest-order (most dangerous) resonances. **b** Evolution of the ground-track spacing for GRACE, shown here as the maximum distance between tracks (in kilometres). There are remarkable differences in this spacing over time, its inverse being the track density, with the maximum spacing (minimum density) at the resonances. Note the lower order of the resonance, the larger distances between tracks (or the lower track density). Note also that the minimum density is not always at the equator but depends on both the resonance order and the orbit inclination while the range of density with latitude is usually large

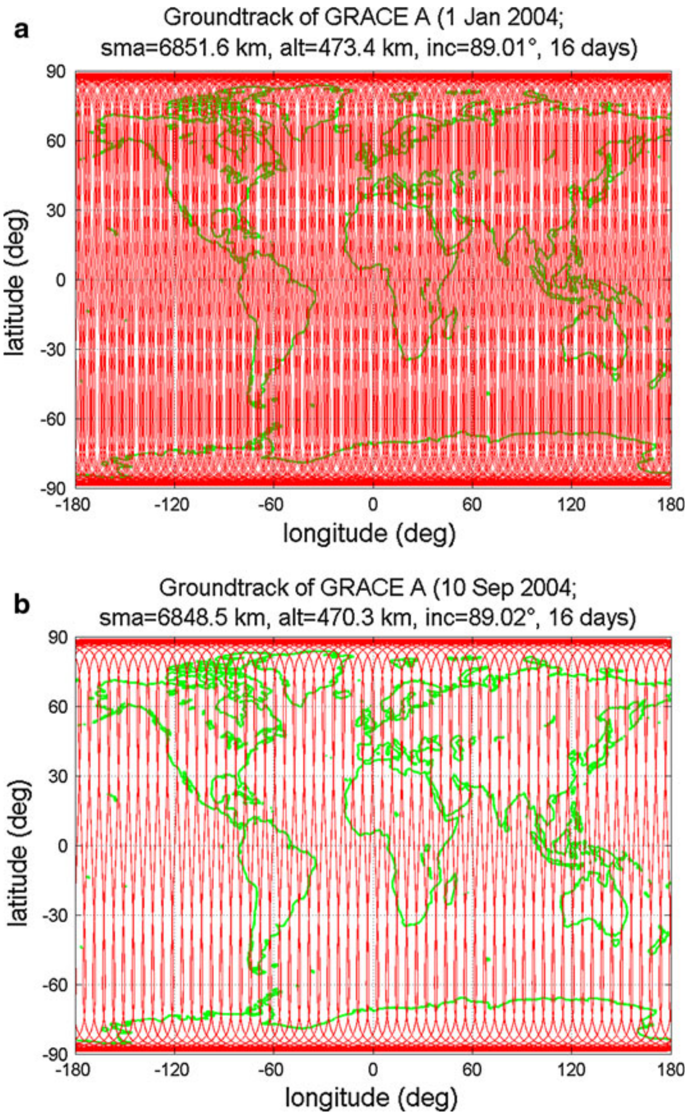

Fig. 9 Ground-tracks of GRACE A a few months before the 61:4 resonance (situation in January 2004, *top figure* **a**) and at the exact 61:4 orbit resonance (September 2004, *bottom figure* **b**). The density D is about 100 km in case **a** and 660 km in case **b**. This density difference correlates with the accuracy changes of the monthly solutions derived from data from GRACE A/B, as is shown in Fig. 7a

7 Application of the GRACE Finding to Orbit Tuning of GOCE

The situation for GOCE is totally different from that for CHAMP (with its few gross orbit altitude changes) and GRACE (with only small manoeuvres to keep the sub-satellites at a constant separation), as both fall freely through the atmosphere. GOCE is kept at a selected height—with as high precision as possible (now better than ±10 m)—by means of an ion motor during the pre-defined observing campaign of the on-board gradiometer. From GRACE we learnt how to choose the appropriate orbit for GOCE by making small changes to its semi-major axis, the changes being known as *fine orbit tuning*. This should avoid any decrease in the accuracy of the geopotential field findings from the gradiometer measurements. Thus, no accuracy decrease should arise here as is possible in a free falling orbit.

GOCE was launched into a near-circular, nearly Sun-synchronous orbit at the initial height of 285 km. During its first, free-decay phase in orbit, the satellite passed through the 16:1 resonance at 268.4 km (as shown in Fig. 10). The effect of this resonance, together with the uncertainty in the solar activity prediction, had a distinct impact on the evolution of the orbital elements. Then, the so-called *measurement operational phases* (MOP) with the gradiometer started. To maintain a near-constant and extremely low altitude for the MOP, the satellite uses an ion-thruster to compensate for atmospheric drag (http://www.esa.int/SPECIALS/GOCE/). To make the ground-track grid dense enough for a proper sampling of the gravitational field, ESA defined, before the launch of GOCE, the constraint for a minimum ground-track repeat period to be 2 months (e.g., Floberghagen et al. 2012).

Bezděk et al. (2009) studied suitable repeat cycles near the 16:1 resonance (point A in Fig. 11). The cycles were found to differ greatly in stability in regard to small perturbations of the satellite's mean altitude and in the evolution of the ground-track coverage. In Fig. 11, points B and C designate two candidate orbital configurations providing dense enough sampling at the end of the 61-day repeat period. The two configurations differ, however, in that the lower one (C) has a 30-day sub-cycle (the point in Fig. 11 labelled

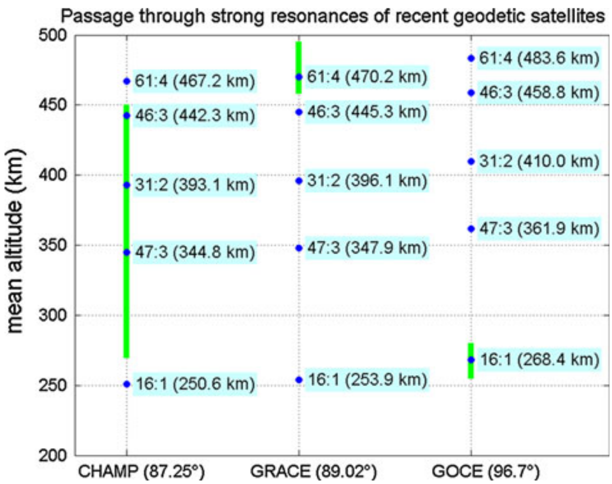

Fig. 10 Passages of CHAMP, GRACE, and GOCE satellites through important low-order orbital resonances

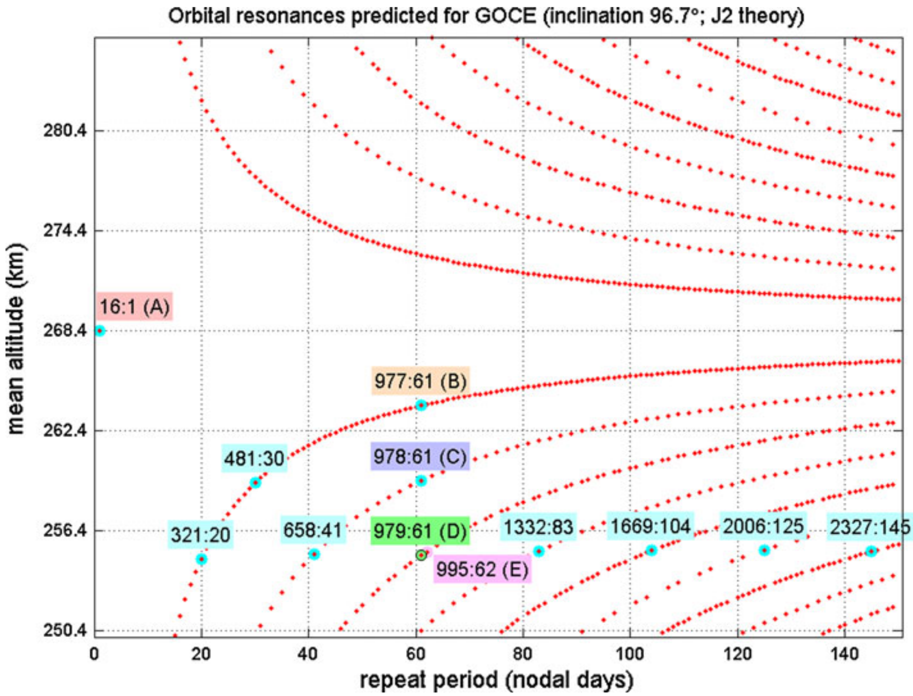

Fig. 11 Evolution of resonances for hypothetical free fall of GOCE. This diagram is used to select a specific high-order resonant orbit. An ion motor on board of GOCE can keep altitude with (at least) 10-m precision

481:30), while the higher one (B) has not. Although the grid of ground-tracks of orbits B and C is of almost the same density, they differ in the way the two ground-track grids are laid down on the Earth' surface. The ground-track grid of orbit B, with no sub-cycles, evolves slowly during the whole repeat period, and a homogeneous global coverage is obtained only after the full 61-day repeat period has elapsed (Fig. 12, panels in the left column). It is different for orbit C, with a second sub-cycle; after the first sub-cycle period of 30 days is over (Fig. 12, panels in the right column), the Earth's surface is already covered by a 'half-dense' global grid of ground-tracks. In this respect, the advantage of repeat orbits with sub-cycles is that, after the sub-cycle repeat period is over, a near regular global coverage of the Earth's surface is achieved, which is, however, less dense. On the other hand, if the altitude of a repeat orbit with sub-cycles is varied by a rather small value (say tens or hundreds of metres), the regularity and/or density of the final ground-track grid might be damaged as there are repeat configurations with differing repeat periods very close in altitude to the chosen one. This is illustrated by the series of the highlighted orbital configurations in Fig. 11, near the altitude of 259.4 km, whose mean altitudes differ by less than 180 m and whose repeat periods have such various values as 20 and 145 days.

At the time of the GOCE launch in March 2009, ESA officially announced the altitude intended for the first measurement phase to be near the repeat orbit (B) with no sub-cycles, on the upper 'branch' of the repeat orbits below the 16:1 resonance (Fig. 11). But due to the extremely low solar activity in 2009, ESA decided that the actual measurement altitude would be a lower 61-day repeat orbit with 20- and 40-day sub-cycles (orbit labelled D in

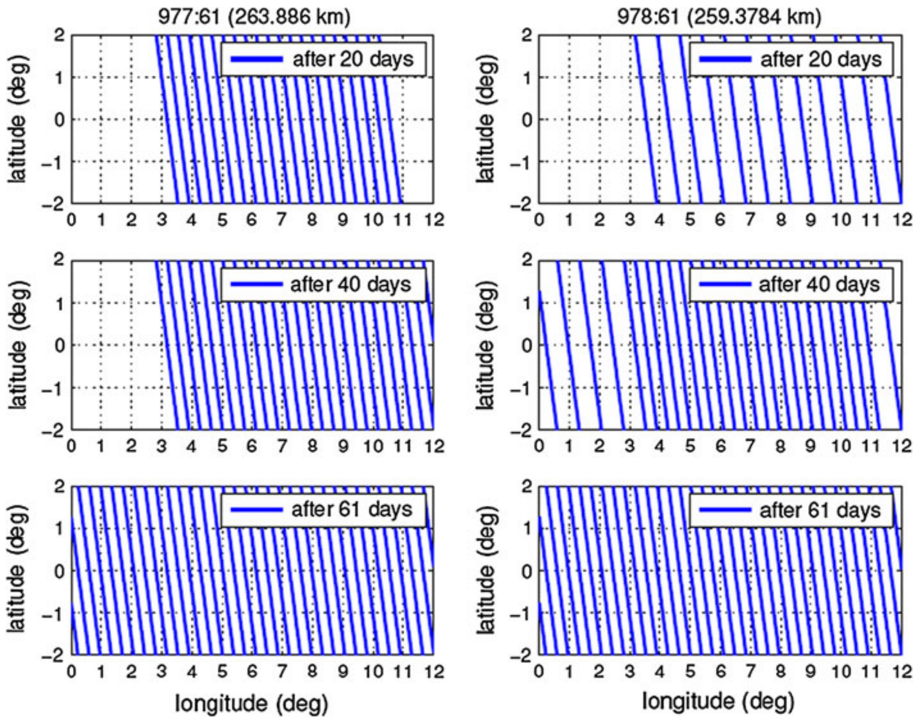

Fig. 12 Temporal evolution of a repeat orbit without a sub-cycle (on the *left*), and with a sub-cycle (on the *right*). Only a small portion of the orbits near the equator is shown

Fig. 11). We analysed the nearby repeat configurations (Bezděk et al. 2010) using a 'full-scale' orbital integrator, and we found that, by a small shift in the mean altitude of 200 m, a 62-day repeat orbit with a somewhat more regular ground-track coverage might be obtained; this is the 995:62 orbit labelled E in Fig. 11.

In Fig. 13 we do not show the ground-tracks over the whole globe, but just in a narrow zone along the equator. In the upper panels, we show a portion of the equator with the ascending ground-tracks; the panels differ in the mean satellite altitude. The ground-track grid of the 61-day repeat orbit (in blue) is regular, corresponding to the close double-peak located at the centre of histograms in the lower panel, with the equatorial gaps spread in the interval between 35 and 45 km. Indeed, in the upper panel of the 61-day orbit, a small irregularity in the longitudinal spacing between the adjacent tracks can be seen. In Fig. 13 we also highlighted the 41-day sub-cycle with the 60 km long equatorial node separations (in red), too long for the required spatial resolution of GOCE. The mean altitude of the 41-day repeat is 100 m above that of the 61-day orbit (see the legend in the lower panel, Fig. 11). Due to the inclusion of all orbital perturbations, the histogram peaks become wider and more complicated; the points corresponding to repeat orbits in Fig. 11 are somewhat blurred and the regular repeat ground-track grids display small irregularities. Here, the concept of fine orbit tuning may be applied. Based only on the simple 'J_2 theory', the ground-track grids of the 61- and 62-day repeat orbits should be practically the same. But with other perturbations included, the ground-track grid of the 62-day orbit (Fig. 13, in green) is more regular, its histogram peak being clearly centred at 40 km. Thus, by making

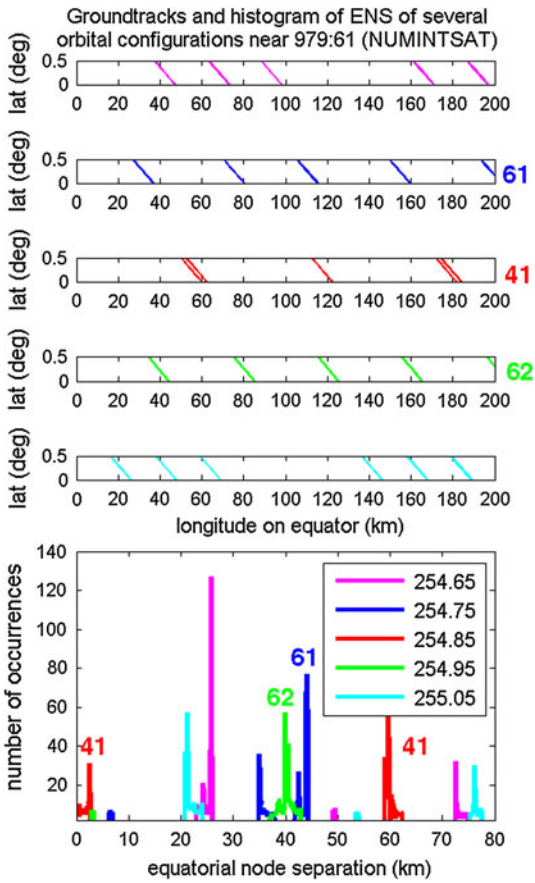

Fig. 13 Histograms of ascending node separation for orbits near the 61-day repeat orbit used in the first measurement operational phase of GOCE

the satellite altitude only 200 m higher, one can obtain the most homogeneous coverage of the Earth surface for the two-month measurement period in the considered altitude range. We see that not only the orbit choice to avoid the 16:1 resonance, but also the proper fine orbit tuning in its vicinity, can significantly affect the quality of scientific data derived from the gradiometer.

8 Planetary Orbiters

The work with GRACE and GOCE can now be applied to planetary orbiters, the tracking of which can be used to improve the gravitational field parameters of the planet. It should be noted that we focus only on the resonance phenomenon and its relationship to the quality of the field parameters; our theoretical study of planetary resonance, therefore, entails no orbit determination.

The question is how the resonance-diagrams will appear for various planetary orbiters; we assume low, circular orbits, and orbiters primarily launched to study the planet's gravitational field. First, we have to use the appropriate values of GM, J_2, R, and $\dot{\nu}$; these are supplied in Table 1, where the values conform to the international standards defined in Seidelmann et al. (2007).

Note that the gravitational fields of Mars, the Moon, and Venus are known to degrees l_{max} of about 95, 100, and 180, respectively (Lemoine et al. 1997, 2001; Marty et al. 2009; Konopliv et al. 1999).

The resonance-diagram for close Mars orbiters (Fig. 14) shows a situation similar to the Earth; we might place a satellite in an orbit in the vicinity of a low-order resonance, such as 13:1, 14:1, or 25:2, but this would lose accuracy in the geopotential analysis. It holds for Mars as for the Earth that $l_{max} \gg \beta$. Thus, an orbiter at a resonance with $\beta \sim$ 12–14 is not appropriate; we should seek an orbit at a high-order resonance. The ground-tracks for the 13:1 resonance of a Mars orbiter are shown in Fig. 15a, to be compared, for example, with those for the 188:15 in Fig. 15b. The actual Mars missions MGS (Mars Global Surveyor, 1998–2006) and ODY (Mars Odyssey, 2002–2008) had orbits with height variations (from the orbit manoeuvres) that led to passing through various higher-order resonances, for example, 188:15, and the choice of heights was satisfactory (but not ideal) from the viewpoint of gravitational field determination.

For future Mars orbiters (in nearly circular orbits), the avoidance of low-order resonances is recommended. Small changes (of a few kilometres) in semi-major axes, whether up or down, could lead to a substantial improvement of parameter accuracy, with negligible extra cost.

The resonant phenomena for the slowly rotating bodies (Table 1) and their orbiters in nearly circular orbits are different from what we are accustomed to for the Earth or Mars. We give here an example, in Figs. 16 a and b, for Venus. For more results (the Moon, Mercury, Mars, and Venus), see Klokočník et al. (2010). The resonance-diagram for slowly rotating planets degenerates to 'stripes' (Fig. 16a). Then, expanding the scale of Fig. 16a, b shows short intervals in semimajor axes that are similar to the graphs we saw for the Earth or Mars. The lowest resonant orders for very low orbits are about (β=) 350, 970, and 3,850 for the Moon, Mercury, and Venus, respectively. Thus, we show that the determination of

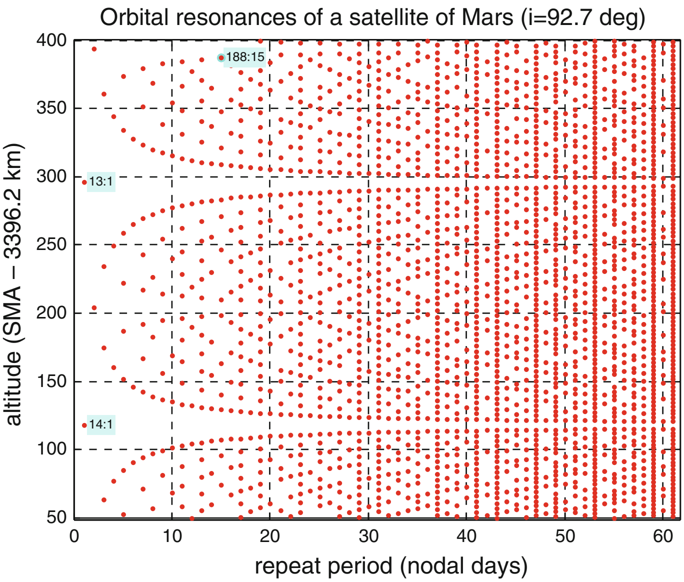

Fig. 14 The resonance-diagram for a Mars orbiter with orbit heights between 50 and 400 km and nominal inclination 92.7°

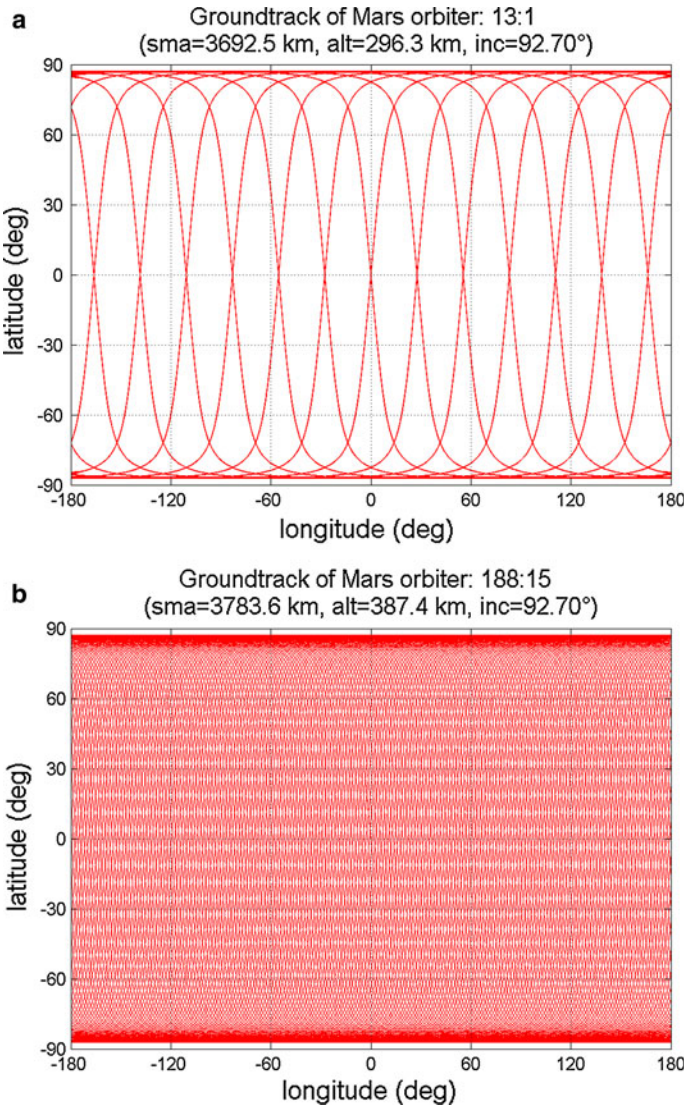

Figs. 15 **a**, **b** Ground-tracks for a Mars orbiter at the 13:1 and 188:15 resonances to compare the track distances and to estimate a possible loss of accuracy due to a hypothetically bad choice of the orbit (too close to the 13:1 or similar low-order resonance); the value *D* at 13:1 is about 1,640 km, while *D* at 188:15 is ~110 km

the gravity fields of these bodies do not lead to the same problem as for the Earth or Mars. For these three bodies, we still have $l_{\max} \ll \beta$. See the example for Venus in Fig. 16b, $\beta = 3{,}851$ or 3,852, which is much more than the highest $l_{\max}$ known till now for the gravity field of Venus (see above), namely 180 (Konopliv et al. 1999).

To summarize Sects. 6–8, a relationship between the ground-track density (dictated by proximity to orbit resonances) and the accuracy of geopotential recovery has been found

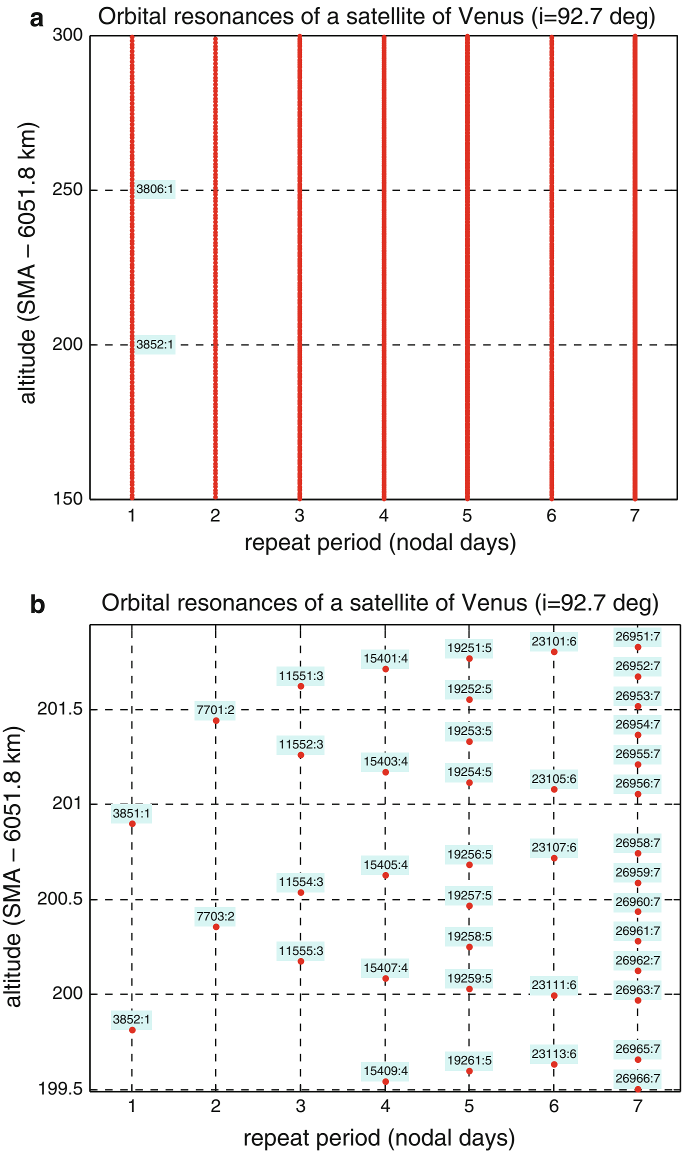

Fig.16 Resonance-diagram (**a**) and its zoom (**b**) for very low and nearly polar orbits of a Venus orbiter

from studying the orbit behaviour of GRACE—*the lower the density, the poorer the accuracy*. The discovery was extended to GOCE, and an extension to other celestial bodies of the solar system was then a logical step. For Mars we found a situation similar to the Earth, and we suggest fine orbit tuning for future close Mars orbiters to achieve maximum gain for the accuracy of gravitational field parameters.

9 Summary

Commensurabilites, or repetitions in the motions of two mutually interacting bodies, result in the physical phenomenon of 'resonance' or amplification of those motions. They are pervasive in nature from astronomy (planetary orbits and ring systems) to engineering (the breakdown of structures under oscillating loads). For physical resonances, we reviewed how the commensurability of the Earth's rotation with the orbital motion of its artificial satellites gave rise to amplified orbit changes facilitating accurate and independent delineation of specific orders of spherical harmonics of the 'lumpy' Earth's gravitational field. These in turn have been used to validate or improve more general models for the parts of those models resonant on these specific orbits. With the advent of repeating Earth satellite orbits conveniently used from the beginning of the space age for communications and all survey purposes, we have recently found that the ones designed to recover the Earth's gravity field from orbit observations can have serious accuracy losses depending on the order of the commensurability (the number of orbit revolutions in a repeat cycle). This order is directly related to the density of ground-tracks in the cycle. High orders (high density) result in accurate recoveries, and low orders (low density) in reduced accuracies. We discussed in detail this last application of commensurate orbits to a few recent and projected gravitational recovery missions for the Earth and other planets. The aim of the planning discussed for these missions (their repeat orbits) was to optimize the recoveries for whatever harmonic field is sought for these planets.

Acknowledgments This work has been supported by grant of ESA (European Space Agency) PECS C 98056. We are grateful to anonymous reviewers for a substantial improvement of our manuscript.

References

Allan RR (1965a) Resonant effects for satellites with nominally constant ground tracks. In: Proc XVIIth Interntl Astronaut Congress, Athens, pp 119–136

Allan RR (1965b) Even tesseral harmonics in the geopotential derived from SYNCOM 2. In: Proc of the international symposium on the use of artificial satellites for geodesy, 2nd, Athens, April

Allan RR (1967a) Resonance effects due to the longitude dependence of the gravitational field of a rotating primary. Planet Space Sci 15:53–76

Allan RR (1967b) Satellite resonance with longitude-dependent gravity—II, effects involving the eccentricity. Planet Space Sci 15:1829–1845

Allan RR (1971) Commensurable eccentric orbits near critical inclination. Celest Mech 3:320–330

Allan RR (1973) Satellite resonance with longitude-dependent gravity—III, inclination changes for close satellites. Planet Space Sci 21:205–225

Balmino G, Reigber Ch, Moynot B (1976) A geopotential model determined from recent satellite observing campaign (GRIM 1). Manuscripta Geodaetica 1:41–69

Bettadpur S, Team L (2006) Status of next generation grace gravity field data products, American Geophysical Union, Fall Meeting, abstract # G11B-03

Bezděk A, Klokočník J, Kostelecký J, Floberghagen R, Gruber C (2009) Simulation of free fall and resonances in the GOCE mission. J Geodyn 48:47–53. doi:10.1016/j.jog.2009.01.007

Bezděk A, Klokočník J, Kostelecký J, Floberghagen R, Sebera J (2010) Some aspects of the orbit selection for the measurement phases of GOCE. In: Proc of the ESA living planet symposium, Bergen, Norway, 28 June–2 July 2010, ESA SP-686

Blitzer L, Boughton M, Kang G, Page R (1962) Effect of ellipticity of the equator on 24-hour nearly circular satellite orbits. J Geophys Res 67:329–335

Bruinsma S, Lemoine J-M, Biancale R, Vales N (2010) CNES/GRGS 10-day gravity field models (release 2) and their evaluation. Adv Space Res 45:587–601. doi:10.1016/j.asr.2009.10.012

Capderou M (2005) Satellite orbits and missions. Springer, Paris, p 364

Colombo O (1983) Altimetry, orbits and tides, NASA Tech. Memo 86180, Goddard Space Flight Center, Greenbelt, Md, 173 pp
ESA (1999) Report for mission selection: the four candidate Earth explorer core missions: GOCE ESA SP-1233
Farless DL (1985)The application of periodic orbits to TOPEX mission design. In: Kaufman B et al (eds) "Astrodynamics", 58, Part I, Adv Astron Sci Am Astronaut Soc, San Diego, pp 13–36
Ferraz-Mello S (1993) Kirkwood gaps and resonant groups. In Milani A et al (eds) Asteroids, Comets, Meteors, IAU publ
Flechtner F, Dahle C, Neumayer KH, König R, Förste Ch (2010) The release 04 CHAMP and GRACE EIGEN gravity models. Adv Technol Earth Sci 2010:41–58. doi:10.1007/978-3-642-10228-8_4
Floberghagen R, Fehringer M, Lamarre D, Muzi D, Frommknecht D, Steiger C, Piñeiro J, da Costa A (2012) Mission design, operation and exploitation of the gravity field and steady-state ocean circulation explorer (GOCE) mission. J Geodesy (GOCE special issue)
Gaposchkin EM (1964) Differential orbit improvement (DOI-3), SAO (Smiths Inst Astrophys Obs) special report # 161, 70 pp, Cambridge
Garfinkel B (1966) Formal solution in the problem of small divisors. Astron J 71:657–669
Gedeon GS, Douglas BC, Palmiter MT (1967) Resonance effects on eccentric satellite orbits. J Astronaut Sci 14:147–157
Gooding RH (1971a) Lumped fifteenth-order harmonics in the geopotential. Nat Phys Sci 231:168–169. doi:10.1038/physci231168a0
Gooding RH (1971b) A recurrence relation for inclination functions. Celest Mech 4:91–98
Gooding RH, King-Hele DG (1989) Explicit form of some functions arising in the analysis of resonant satellite orbits. Proc Roy Soc Lond A422:241–259
Gooding RH, Wagner CA (2008) On the inclination functions and a rapid stable procedure for their evaluation together with derivatives. Celest Mech Dyn Astron 101(# 3):247–272. doi:10.1007/s10569-008-9145-6
Gooding RH, Wagner CA (2010) On a Fortran procedure for rotating spherical-harmonic coefficients. Celest Mech Dyn Astron 108:95–106. doi:10.1007/s10569-010-9293-3
Gooding RH, Wagner CA, Klokočník J, Kostelecký J, Reigber C (2004) CHAMP and resonances. In: Reigber C, Luhr H, Schwintzer P, Wickert J (eds) Earth observation with CHAMP, results from three years in orbit. Springer, Berlin, pp 101–107
Gooding RH, Wagner CA, Klokočník J, Kostelecký J, Gruber C (2007) CHAMP and GRACE resonances, and the gravity field of the Earth. Adv Space Res 39 (# 10):1604–1611. ISSN 0273-1177
Hugentobler U, Beutler G (1993) In: Kurzynska K (ed) Proceedings of the conference on astrometry and celestial mechanics, Poznań, pp 347–352
Hugentobler U, Ploner M, Schildknecht T, Beutler G (1999) Determination of resonant geopotential terms using optical observations of geostationary satellite. Adv Space Res 23(# 4):767–770. doi:10.1016/S0273-1177(99)00153-2
Kaula WM (1966) Theory of satellite geodesy, Blaisdell Publ. Comp., Waltham (Mass.), Toronto, London (reedited in 2001); re-issued as posthumous paperback in 2003
King-Hele DG (1972) Poems and trixies, The Mitre Press London; For Imre Izsak, Earth shaper, p 9
King-Hele DG (1992) A tapestry of orbits. Cambridge University Press, Cambridge
King-Hele DG, Walker DMC (1989) Evaluation of 15th- and 30th-order geopotential harmonic coefficients from 26 resonant satellite orbits. Planet Space Sci 37:805–823. doi:10.1016/0032-0633(89)90132-3
King-Hele DG, Walker DMC, Gooding RH (1974) Evaluation of harmonics in the geopotential of order 15 and odd degree. Planet Space Sci 22:1349–1373. doi:10.1016/0032-0633(74)90035-X
Klokočník J (1976) Changes in the inclination of a close earth satellite due to orbital resonances. Bull Astron Inst Czechoslov 27:287–295
Klokočník J (1979) 15th-order resonance of Interkosmos 11, analysis of the inclination. Bull Astron Inst Czechoslov 30:214–219
Klokočník J (1988) Geopotential research mission: a contribution to assessment of orbit accuracy, orbit determination and gravity field modelling, presented at Intercosmos conf. of 6th section, Szentendre (1987), publ. In: Bulletin of Astronomical Institutes of Czechoslovakia 38:45–67
Klokočník J, Kostelecký J (1981) A possible contribution to the Earth model "GRIM 3", Edice VUGTK 5, #6, 18 pages, Zprávy a pozorování Geodet. Obs. Pecný (in Czech), report of Res Inst Geodesy, Cartogr and Topogr, Zdiby
Klokočník J, Kostelecký J, Gooding RH (2003) On fine orbit selection for particular geodetic and oceanographic missions involving passage through resonances. J Geodesy 77:30–40. doi:10.1007/s00190-002-0276-3

Klokočník J, Kostelecký J, Wagner CA (2008a) Improvement in the radial accuracy of altimeter satellite orbits due to the geopotential. Earth Sci Rev 91(1–4):106–120

Klokočník J, Wagner CA, Kostelecký J, Bezděk A, Novák P, McAdoo D (2008b) Variations in the accuracy of gravity recovery due to ground track variability: GRACE, CHAMP, and GOCE. J Geodesy 82:917–927. doi:10.1007/s00190-008-0222-0

Klokočník J, Bezděk A, Kostelecký J, Sebera J (2010) Orbit tuning of planetary orbiters for accuracy gain in gravity-field mapping. J Guid Control Dyn 33:853–861

Konopliv AS, Banerdt WB, Sjogren WL (1999) Venus gravity: 180th degree and order model. Icarus 139 (# 1):3–18. doi:10.1006/icar.1999.6086

Kostelecký J (1985) Recurrence Relations for the Normalized Inclination Function. Bull Astron Inst Czechoslov 36:242–246

Kostelecký J, Klokočník J (1979) 30th-order harmonics from resonant inclination variations of ten satellites. Bull Astron Inst Czechoslov 30:45–51

Kostelecký J, Klokočník J (1983) Collocations and the thirtieth order resonant harmonics, Planet Space Sci 31:829–841; doi:10.1016/0032-0633(83)90136-8, see also abstract in Observations Artif Satel Earth 18:227–231, Pol Acad Sci, Warsaw, 1978

Kostelecký J, Klokočník J, Kalina Z (1986) Computation of normalized inclination function to high degree for satellites in resonances. Manuscripta Geodaetica 11:293–304

Lála P, Kostelecký J (1980) PRIOR. A computer program for determination of orbits, Edice VUGTK 5, Zprávy a pozorování Geodet. Obs. Pecný, pp 3–19

Laplace PS (1825) Traité de Mécanique Céleste, 3rd Volume, pp 27–31, Gauthier-Villars, Paris, reedition 1878

Lefebvre M, Vincent R (1988) An orbit scenario fitting most of constraints of altimeter, SAR, and Scat-erometer Missions, ERS 1 Sampling Capabilities, French PAF for ERS-1, CNES Techn Rep, Toulouse

Lemoine FG, Smith DE, Zuber MT, Neumann GA, Rowlands DD (1997) A 70th degree lunar gravity model (GLGM-2) from clementine and other tracking data. J Geophys Res 102(E7):16339–16359. doi: 10.1029/97JE01418

Lemoine FG, Smith DE, Rowlands DD, Zuber MT, Neumann GA, Chinn DS (2001) An improved solution of the gravity field of mars (GMM-2B) from mars global surveyor. J Geophys Res 106(E10):23359–23376. doi:10.1029/2000JE001426

Marty JC, Balmino G, Duron J, Rosenblatt P, Le Maistre S, Rivoldini A, Dehant V, Van Hoolst T (2009) Martian gravity field model and its time variations from MGS and odyssey data. Planet Space Sci 57:350–363. doi:10.1016/j.pss.2009.01.004

Moritz H (1980) Advanced physical geodesy, Wichman Verlag, Karlsruhe, Abacus Press, Tunbridge, Wells, Kent

Murphy JP, Victor EL (1968) A determination of the second and fourth order sectorial harmonics in the geopotential from the motion of 12-hour satellites. Planet Space Sci 16:195–204

Murray CD, Dermott SF (1999) Solar system dynamics, Cambridge University Press (reprint in 2001). http://ssdbook.maths.qmul.ac.uk/

Nobili AM (1993) An international campaign of optical observations of geosynchronous satellites (COG-EOS): scientific aims and organization. Reprint from CSTG Bull 1987, 9:19–30. A collection of papers from workshop of COGEOS in Zaragoza, Spain

Pavlis NK, Holmes SA, Kenyon SC, Factor JK (2008) An earth gravitational model to degree 2160: EGM2008, EGU General Assembly 2008, Vienna, Austria, Geophysical Research Abstracts, vol 10, Abstract EGU 2008-A-01891

Reigber Ch (1973) Generalized Fourier analysis of resonant orbits. In: Rycroft MJ, Runcorn SK (eds) COSPAR Space Research XIII, Proc, Akademie-Verlag Berlin, pp 3–10

Reigber Ch, Balmino G (1975) Even and odd degree 13th-order harmonics from analysis of stable near resonant satellite orbits, in Die Arbeiten des SFB 78 TU Munchen in 1975, Bayer. Kom Interntl Erdmessung, Bayer. Akad Wiss Heft 35, Munich, Germany; see also 1976 GRGS Bull. # 15, pp 1–46, Toulouse, France

Reigber Ch, Balmino G (1976) 14th-order harmonics from analysis of mean longitude of resonant satellites, presented at OMWG 1, paper I.2.5, XIXth COSPAR meeting, June, Philadelphia, USA

Reigber Ch, Rummel R (1978) 12th-order harmonics from resonant perturbations of satellites using non-homogeneous weight functions, presented at 2nd Intrntl Symp “The Use of Artif Satell for Geodesy and Geodynamics”, May 29–June 3, Athens, Greece

Reigber Ch, Klokočník J, Li H, Flechtner F (1988) Contribution to ERS-1, Orbit Dossier, German PAF for ERS-1, DGFI Rep, Munich, Germany

Reigber Ch, Lühr H, Schwintzer P (eds) (2003) First CHAMP mission results for gravity, magnetic and atmospheric studies. Springer, Berlin

Reigber Ch, Lühr H, Schwintzer P, Wickert J (eds) (2005) Earth observations with CHAMP, results from three years in orbit. Springer, Berlin
Risbo T (1996) Fourier transform summation of Legendre series and D-functions. J Geodesy 70:383–396. doi:10.1007/BF01090814
Rummel R, Yi W, Stummer C (2011) GOCE gravitational gradiometry. J Geodesy 85:777–790. doi: 10.1007/s00190-011-0500-0
Schneider M (1973) Orbit determination by solving a boundary value problem. In: Tapley BD, Szebehely V (eds) Recent advances in dynamical astronomy. Reidel, Dordrecht, pp 426–428
Seidelmann PK, Archinal BA, A'hearn MF, Conrad A, Consolmagno GJ, Hestroffer D, Hilton JL, Krasinsky GA, Neumann G, Oberst J, Stooke P, Tedesco EF, Tholen DJ, Thomas PC, Williams IP (2007) Repot of the IAU/IAG Working Group on cartographic coordinates and rotational elements: 2006. Celest Mech Dyn Astron 98(3):155–180. doi:10.1007/s10569-007-9072-y
Sneeuw NJ (1992) Representation coefficients and their use in satellite geodesy, Manuscripta Geodaetica 17:117–123. http://books.google.com/books/id=ZcodAQAAIAAJ
Tapley BD, Bettadpur S, Watkins M, Reigber C (2004) The gravity recovery and climate experiment: mission overview and early results, Geophysical Research Letters 31: (# 9), L09607; doi: 10.1029/2004GL010020
Wagner CA (1965) A determination of Earth's equatorial ellipticity from seven months of Syncom 2 longitude drift. J Geophys Res 70:1566–1568
Wagner CA (1968a) Determination of low-order resonant gravity harmonics from the drift of two Russian 12-hour satellites. J Geophys Res 73:4661–4674
Wagner CA (1968b) Combined solution for low degree longitude harmonics of gravity from 12- and 24-hour satellites. J Geophys Res 73:7651–7660
Wagner CA (1973) Zonal gravity harmonics from long satellite arcs by a semi-numeric method. J Geophys Res 78:3271–3280
Wagner CA (1974) Eleventh-order geopotential resonance on the orbit of Vanguard 3. J Geophys Res 79:3335–3341
Wagner CA (1979) Gravitational spectra from the tracking of planetary orbiters. J Geophys Res 84(B12):6891–6908. doi:10.1029/JB084iB12p06891
Wagner CA (1983) The accuracy of the low-degree geopotential: implications for ocean dynamics. J Geophys Res 88(6):5083–5090
Wagner CA (1991) A prograde Geosat exact repeat mission? J Astron Sci 39: (#.3), p 316, Eq. (16)
Wagner CA, Douglas BC (1969) Perturbations of existing resonant satellites. Planet Space Sci 17:1505–1517
Wagner CA, Douglas BC (1970) Resonant satellite geodesy by high speed analysis of mean Kepler elements. Dyn Satell, Springer, pp 130–137
Wagner CA, Klosko SM (1975) 15th order dragged resonance on the orbit of TETR 3. Planet Space Sci 23:541–549
Wagner CA, Klosko SM (1977) Gravitational harmonics from shallow resonant orbits. Celest Mechan 16:143–163
Wagner CA, Lerch FJ (1978) The accuracy of geopotential models. Planet Space Sci 26:1081–1140
Wagner CA, McAdoo DC, Klokočník J, Kostelecký J (2005) Degradation of grace monthly Geopotentials in 2004 explained. EOS Trans AGU 86(18), J Assem Suppl, abstract G23B04
Wagner CA, McAdoo D, Klokočník J, Kostelecký J (2006) Degradation of geopotential recovery from short repeat-cycle orbits: application to GRACE monthly fields. J Geodesy 80:94–103. doi: 10.1007/s00190-006-0036-x
Wakker KF, Klokočník J, Kostelecký J, Sehnal L (1981) Analysis of inclination variations of the first Netherlands satellite. Bull Astron Inst Czechoslov 32:168–178
Walker DMC (1981) Analyses of the US Navy orbits of 1963-24B and 1974-34A at 15th-order resonance. Geophys J Royal Astron Soc 67 (# 1):1–18. doi:10.1111/j.1365-246X.1981.tb02728.x
Weigelt M, Sideris MG, Sneeuw N (2009) On the influence of the ground tracks on the gravity field recovery from high-low satellite-to-satellite tracking missions: CHAMP monthly gravity field recovery using the energy balance approach revisited. J Geodesy 83:1131–1143. doi:10.1007/s00190-009-0330-5
Wilson C (1985) The great inequality of Jupiter and Saturn: from Kepler to Laplace. Arch Hist Exact Sci 33:15–290. doi:10.1007/BF00328048